Explicit integrators for the magnetized equations of motion in Particle in Cell codes

Explicit integrators for the magnetized equations of motion in Particle in Cell codes

L. Patacchini and I.H. Hutchinson

Plasma Science and Fusion Center, MIT Cambridge, Massachusetts, 02139, USA

Abstract

The development of a new orbit integrator (called Cyclotronic integrator) particularly suitable for magnetized Particle in Cell codes where the Larmor angular frequency Ω is larger than any other characteristic frequencies is presented. This second order scheme, shown to be symplectic when the background magnetic field is static and uniform, is a bridge between the well-known Boris push in the limit of small time steps ($\Omega\Delta t \ll 1$) and the Spreiter and Walter Taylor expansion algorithm in the opposite limit ($\Omega\Delta t \gg 1$). The Boris and the Cyclotronic integrators' performances are investigated in terms of linear stability, local accuracy and conservation properties; in both uniform and two-dimensional magnetic field geometries. It is shown that in a uniform magnetic field and provided $\Omega\Delta t \lesssim 1$, the Cyclotronic integrator necessarily outperforms the two other alternatives.

1 Introduction

The Boris integration scheme [1], designed to solve the single particle equations of motion in electric and magnetic fields

$$\left\{ \begin{array}{rcl} \dot{\mathbf{x}} & = & \mathbf{v} \\ m\dot{\mathbf{v}} & = & Q\left(\mathbf{E}+\mathbf{v}\wedge\mathbf{B}\right), \end{array} \right. \tag{1}$$

is perhaps the most widely used orbit integrator in explicit Particle In Cell (PIC) simulations of plasmas. In Eqs (1) $\mathbf{x}$ and $\mathbf{v}$ are the particle position and velocity, m its mass and Q its charge. The idea of the Boris integrator is to offset $\mathbf{x}$ and $\mathbf{v}$ by half a time-step ($\Delta t/2$), and update them alternatively using the following *Drift* and *Kick* operators:

$$\mathrm{D}(\Delta t) \;:=\; \mathbf{x}' - \mathbf{x} = \Delta t\mathbf{v} \tag{2}$$

$$\mathrm{K}(\Delta t) \;:=\; \mathbf{v}' - \mathbf{v} = \Delta t\frac{Q}{m}[\mathbf{E}(\mathbf{x}') + \frac{\mathbf{v}'+\mathbf{v}}{2}\wedge\mathbf{B}(\mathbf{x}')]. \tag{3}$$

Although seemingly implicit (the right hand side of Eq. (3) contains both $\mathbf{v}$ and $\mathbf{v}'$, the velocities at the beginning and end of the step), K can easily be inverted and the

scheme is in practice explicit as will be discussed in more detail in Section 2.1. The reasons for Boris scheme's popularity are twofold.

It must first be recognized that the algorithm is extremely simple to implement, and offers second order accuracy while requiring only one force (or field) evaluation per step. Other integrators such as the usual or midpoint second order Runge-Kutta [2] require two field evaluations per step, thus considerably increasing the computational cost. The second reason is that for stationary electric and magnetic fields, the errors on conserved quantities such as the energy or the canonical angular momentum when the system is axisymmetric, are bounded for an infinite time (The error on those quantities is second order in Δt as is the scheme). Those conservation properties, usually observed on long-time simulations of periodic or quasi-periodic orbits, are characteristic of time-reversible integrators [3].

The Boris scheme has a weak point however; it requires a fine resolution of the Larmor angular frequency $\Omega = Q|\mathbf{B}|/m$, typically $\Omega\Delta t \lesssim 0.1$ [4, 5]. After a brief review of the Boris push, we present a novel integrator subject to a much weaker Larmor constraint. This scheme, called Cyclotronic integrator, splits the equations of motion (1) by taking advantage of the fact that in a uniform magnetic field and zero electric field the particle trajectory has a simple analytic form. Using this method, it is shown that provided the Larmor frequency is much higher than any other characteristic frequencies of the problem, the time step is only limited by stability considerations, typically leading to $\Omega\Delta t \lesssim 1$. If the background magnetic field is uniform, in addition to being time-reversible the Cyclotronic integrator is shown to be symplectic [6]; in other words it preserves the geometric structure of the Hamiltonian flow. Those different schemes are benchmarked on test problems involving uniform and 2D magnetic fields.

Spreiter and Walter [7] previously attempted to relax the Larmor constraint, and developed a "Taylor expansion algorithm" for the static and uniform magnetic field regimes that we compare with the Cylotronic integrator. While both integrators have almost identical short-term performances, the Taylor expansion algorithm suffers from non time-reversibility and unconditional unstability. We therefore show that it should be preferred to the Cyclotronic integrator only when $\Omega\Delta t \gtrsim 1$.

2 Derivation of Boris and Cyclotronic integrators

2.1 Boris integrator

The Boris integrator is a time-splitting method for Eqs (1): the equations of motion are separated in two parts that are successively integrated in a Verlet form, in other words

$$\begin{pmatrix} \mathbf{x} \\ \mathbf{v} \end{pmatrix}(t+\Delta t) = \mathrm{D}(\Delta t/2)\cdot\mathrm{K}(\Delta t)\cdot\mathrm{D}(\Delta t/2)\begin{pmatrix} \mathbf{x} \\ \mathbf{v} \end{pmatrix}(t), \tag{4}$$

where the Drift and Kick operators (D and K) are defined in Eqs (2,3). If $\overline{\overline{R}}_{\boldsymbol{\Delta\varphi}}$ denotes a rotation of characteristic vector

$$\boldsymbol{\Delta\varphi} = 2\tan^{-1}(\frac{\Delta t}{2}\Omega)\frac{\mathbf{B}}{B} \sim \Omega\Delta t\frac{\mathbf{B}}{B}, \tag{5}$$

$\mathrm{K}(\Delta t) := \mathbf{v} \to \mathbf{v}'$ can be split in the following way [1]

$$\mathrm{K}(\Delta t) := \left\{ \begin{array}{rcl} \mathbf{v}^* & = & \mathbf{v} + \frac{Q\mathbf{E}\Delta t}{2m} \\ \mathbf{v}^{**} & = & \overline{\overline{R}}_{\mathbf{\Delta}\varphi}\mathbf{v}^* \\ \mathbf{v}' & = & \mathbf{v}^{**} + \frac{Q\mathbf{E}\Delta t}{2m}. \end{array} \right. \tag{6}$$

Eqs (2,6) readily show that the Boris integrator is time-reversible. Indeed the Drift operator does not act on the particle velocity, and the Kick operator does not act on the position. In PIC codes it is customary to define the position and velocity with half a time-step of offset, which amounts to concatenating the two adjacent $\mathrm{D}(\Delta t/2)$ from successive steps in Eq. (4).

A popular variant of this integrator (known as the "tan" transformation [1]), second order in Δt , consists in letting $\mathbf{\Delta}\varphi = \Omega\Delta t\frac{\mathbf{B}}{B}$ in Eq. (6). Regardless of the form used for $\mathbf{\Delta}\varphi$ however, the Drift operator (2) requires $\Omega\Delta t \ll 1$, which is a severe limitation if the other characteristic frequencies (Such as the quadrupole harmonic frequency ω_0 introduced in Section 3) are much smaller than Ω.

2.2 Symplectic and time-reversible integration

Time-reversible integrators contain the subclass of symplectic schemes, which has recieved considerable attention in the last decades in particular in connection with astrodynamics [8] and accelerator physics [9].

The fundamental idea behind symplectic integration of (systems of) Ordinary Differential Equations (ODEs) is to ensure that the chosen scheme is a canonical map, in other words that there exists canonical coordinates $(\mathbf{q}, \mathbf{p})$ related to the physical variables $(\mathbf{x}, \mathbf{v})$ such that the flow $Z(\tau) = (\mathbf{q}, \mathbf{p})(\tau)$ derives from a Hamiltonian $\tilde{\mathrm{H}}$:

$$\frac{\mathrm{d}\mathbf{p}}{\mathrm{d}t} = -\nabla_{\mathbf{q}}\tilde{\mathrm{H}} \qquad \frac{\mathrm{d}\mathbf{q}}{\mathrm{d}t} = \nabla_{\mathbf{p}}\tilde{\mathrm{H}}, \tag{7}$$

in which case there exists a Liouville operator $\Psi_{\tilde{\mathrm{H}}}$ such that

$$\frac{\mathrm{d}Z}{\mathrm{d}t} = \{Z, \tilde{\mathrm{H}}(Z)\} = \Psi_{\tilde{\mathrm{H}}}Z \tag{8}$$

or equivalently

$$\forall\tau \in \mathbf{R} \quad z(\tau) = e^{\tau\Psi_{\tilde{\mathrm{H}}}}Z(0), \tag{9}$$

where $\{.,.\}$ stands for the Poisson bracket. Indeed if the original ODEs derive from a Hamiltonian $\mathrm{H}(\mathbf{q}, \mathbf{p})$, one can show that the Hamiltonian from which the flow of a consistent n^{th} order symplectic integrator derives takes the form: $\tilde{\mathrm{H}}(\mathbf{q}, \mathbf{p}) = \mathrm{H}(\mathbf{q}, \mathbf{p}) + \delta\mathrm{H}(\mathbf{q}, \mathbf{p}, \Delta t)$, where $\delta\mathrm{H} = O(\Delta t^n)$ [10]. Because the integrator exactly preserves $\tilde{\mathrm{H}}$ and its integral invariants, it is expected to conserve slightly modified expressions of the integral invariants of H. Hence no secular drift in the original problem's energy or integral invariants is to occur. For a more complete introduction on symplectic integration avoiding unnecessary mathematical formalism, the reader is referred to Ref. [6].

The Boris integrator is known for its outstanding conservation properties. However as pointed out by Stolz *et al.* [11], there is no guarantee that it is symplectic. It is nonetheless time-reversible, and it has been shown under very reasonable assumptions that this condition is sufficient to explain the absence of secular drift in the conserved quantities, provided the orbit we integrate is periodic or quasi-periodic [3].

2.3 Cyclotronic integrator

The time independent Hamiltonian for single particle motion in the presence of a uniform background magnetic field $\mathbf{B} = B\mathbf{e_z}$ can easily be written in cylindrical coordinates:

$$\mathrm{H}(\mathbf{q},\mathbf{p}) = \frac{p_\rho^2}{2m} + \frac{p_z^2}{2m} + \frac{1}{2m}\left(\frac{p_\varphi}{\rho} - QA_\varphi(\rho,z)\right)^2 + Q\phi(\mathbf{q}), \tag{10}$$

where the generalized momentum $\mathbf{p}$ is given by

$$\begin{cases} p_z &= & m\dot{z} \\ p_\rho &= & m\dot{\rho} \\ p_\varphi &= & m\rho^2\left(\dot{\varphi} + Q\frac{A_\varphi}{m\rho}\right) \end{cases} \tag{11}$$

and $\mathbf{q} = (z,\rho,\varphi)$. The vector potential $\mathbf{A}$ satisfies $\nabla \wedge \mathbf{A} = B\mathbf{e_z}$ and is chosen to be $\mathbf{A} = \frac{B\rho}{2}\mathbf{e}_\varphi$, while $\mathbf{E} = -\nabla\phi$.

The flow deriving from the full Hamiltonian H in Eq. (10) is not integrable. It is however possible to rewrite H as $\mathrm{H} = \mathrm{H}_1 + \mathrm{H}_2$ where the flows associated with $\mathrm{H}_{1,2}$ are exactly integrable for any time-step Δt as follows:

- Drift part: $\mathrm{H}_1(\mathbf{q},\mathbf{p}) = \frac{p_\rho^2}{2m} + \frac{p_z^2}{2m} + \frac{1}{2m}\left(\frac{p_\varphi}{\rho} - QA_\varphi(\rho,z)\right)^2$
  Uniform helical motion around $\mathbf{B}$ with angle $\mathbf{\Delta}\varphi = \Omega\Delta t\frac{\mathbf{B}}{B}$.
- Kick part: $\mathrm{H}_2(\mathbf{q},\mathbf{p}) = Q\phi(\mathbf{q})$
  Momentum increase of vector $-Q\nabla\phi\Delta t$.

Using the Baker Campbell Hausdorff formula [6], one can show that

$$e^{\Delta t\Psi_H} = e^{(\Delta t/2)\Psi_{\mathrm{H}1}} \cdot e^{\Delta t\Psi_{\mathrm{H}2}} \cdot e^{(\Delta t/2)\Psi_{\mathrm{H}1}} + O(\Delta t^3) \tag{12}$$

A second order symplectic integrator for H is therefore

$$A(\Delta t) = e^{(\Delta t/2)\Psi_{\mathrm{H}1}} \cdot e^{\Delta t\Psi_{\mathrm{H}2}} \cdot e^{(\Delta t/2)\Psi_{\mathrm{H}1}} \tag{13}$$

or its conjugate $\bar{A}(\Delta t) = e^{(\Delta t/2)\Psi_{\mathrm{H}2}} \cdot e^{\Delta t\Psi_{\mathrm{H}1}} \cdot e^{(\Delta t/2)\Psi_{\mathrm{H}2}}$.

In the absence of electric field (And of course for a uniform magnetic field) the Cyclotronic integrator is exact regardless of Δt. One can straightforwardly show that it is second order accurate even for complicated magnetic field geometries, in which case one must, at each time-step, consider the rotations described in Eq. (14) to be about the local magnetic axis. However in this case it is not symplectic nor time-reversible.

A practical implementation in Cartesian coordinates of the cyclotronic integrator ready to use in PIC codes where $\mathbf{B} = B\mathbf{e_z}$ is given by Eqs (15,16), where $\mathrm{D}(\Delta t)$ and $\mathrm{K}(\Delta t)$ are the Drift and Kick operators in $(\mathbf{x}, \mathbf{v})$ space corresponding to $\exp(\Delta t \Psi_{\mathrm{H1}})$ and $\exp(\Delta t \Psi_{\mathrm{H2}})$ in $(\mathbf{q}, \mathbf{p})$ space. With $\mathbf{v}$ and $\mathbf{x}$ offset by half a time-step, applying both operators results in $(\mathbf{x}, \mathbf{v}) \to (\mathbf{x}', \mathbf{v}') \to (\mathbf{x}'', \mathbf{v}'')$.

1. Drift

$$\mathrm{D}(\Delta t) := \left\{ \begin{array}{rcl} z' & = & z + v_z \Delta t \\ (x,y)' & = & (x,y)_c + R_{\boldsymbol{\Delta}\varphi}\left((x,y) - (x,y)_c\right) \\ (v_x, v_y)' & = & R_{\boldsymbol{\Delta}\varphi}(v_x, v_y) \end{array} \right. \tag{14}$$

$(x,y)_c(t)$ being the center of the current Larmor radius. More explicitly:

$$\mathrm{D}(\Delta t) := \left\{ \begin{array}{rcl} z' - z & = & v_z \Delta t \\ x' - x & = & \frac{v_y - v_y \cos(\Omega\Delta t) + v_x \sin(\Omega\Delta t)}{\Omega} \\ y' - y & = & \frac{-v_x + v_x \cos(\Omega\Delta t) + v_y \sin(\Omega\Delta t)}{\Omega} \\ v_x' & = & v_x \cos(\Omega\Delta t) + v_y \sin(\Omega\Delta t) \\ v_y' & = & v_y \cos(\Omega\Delta t) - v_x \sin(\Omega\Delta t) \end{array} \right. \tag{15}$$

2. Kick:

$$\mathrm{K}(\Delta t) := \mathbf{v}'' - \mathbf{v}' = -Ze\nabla\phi(\mathbf{x}')\Delta t. \tag{16}$$

3 Linear stability

3.1 Linear electric fields

In addition to being consistent with the original equation, it is desirable that an integration scheme be stable. However proving that this is the case for arbitrary ODEs and initial conditions is in general not feasible, and stability properties are therefore usually assessed on linearized forms of the propagation equations. That an orbit integrator be linearly stable for any particle position and time is a necessary condition for its stability in the presence of an arbitrary potential distribution, and is in practice sufficient.

Let us consider a uniform background magnetic field $\mathbf{B} = B\mathbf{e_z}$, and an ideal quadrupole potential distribution ($\nabla^2\phi = 0$):

$$\phi(\mathbf{r}) = \epsilon\left(\frac{1}{2}\omega_{0x}^2 x^2 + \frac{1}{2}\omega_{0y}^2 y^2 - \frac{1}{2}(\omega_{0x}^2 + \omega_{0y}^2) z^2\right) \tag{17}$$

where $\epsilon = \pm 1$.

Because transverse and axial dynamics are decoupled, we can concentrate on the transverse motion and treat the problem as two-dimensional; we therefore write the position and velocity evolution between two time-steps as

$$\begin{pmatrix} x \\ y \\ v_x\Delta t \\ v_y\Delta t \end{pmatrix}^{n+1} = A \begin{pmatrix} x \\ y \\ v_x\Delta t \\ v_y\Delta t \end{pmatrix}^{n}, \tag{18}$$

where A is a linear operator depending on the dimensionless quantities $\epsilon\omega_{0x,y}\Delta t$ and $\Omega\Delta t$. The integration scheme is stable if and only if

$$\max(|\mathrm{Sp}(A)|) \leq 1 \tag{19}$$

For the Cyclotronic integrator, the operator A_{Cyclo} to be used in Eq. (18) corresponding to Eq. (13) is:

$$A_{\mathrm{Cyclo}} = \mathrm{D}_{\mathrm{Cyclo}} \cdot \mathrm{K}_{\mathrm{Cyclo}} \cdot \mathrm{D}_{\mathrm{Cyclo}} \tag{20}$$

where $\mathrm{D}_{\mathrm{Cyclo}}$ is the operator associated with the half Drift (c.f. Eq. (15)):

$$\mathrm{D}_{\mathrm{Cyclo}} = \begin{pmatrix} 1 & 0 & \frac{\sin(\Omega\Delta t/2)}{\Omega\Delta t} & \frac{1-\cos(\Omega\Delta t/2)}{\Omega\Delta t} \\ 0 & 1 & -\frac{1-\cos(\Omega\Delta t/2)}{\Omega\Delta t} & \frac{\sin(\Omega\Delta t/2)}{\Omega\Delta t} \\ 0 & 0 & \cos(\Omega\Delta t/2) & \sin(\Omega\Delta t/2) \\ 0 & 0 & -\sin(\Omega\Delta t/2) & \cos(\Omega\Delta t/2) \end{pmatrix} \tag{21}$$

and $\mathrm{K}_{\mathrm{Cyclo}}$ with the Kick (c.f. Eq. (16)):

$$\mathrm{K}_{\mathrm{Cyclo}} = \begin{pmatrix} 1 & 0 & 0 & 0 \\ 0 & 1 & 0 & 0 \\ -\epsilon\omega_{0x}\Delta t & 0 & 1 & 0 \\ 0 & -\epsilon\omega_{0y}\Delta t & 0 & 1 \end{pmatrix} \tag{22}$$

For the Boris integrator, the operator A_{Boris} corresponding to Eq. (4) is:

$$A_{\mathrm{Boris}} = \mathrm{D}_{\mathrm{Boris}} \cdot \mathrm{K}_{\mathrm{Boris}} \cdot \mathrm{D}_{\mathrm{Boris}} \tag{23}$$

where $\mathrm{D}_{\mathrm{Boris}}$ is the operator associated with the half Drift:

$$\mathrm{D}_{\mathrm{Boris}} = \begin{pmatrix} 1 & 0 & 1/2 & 0 \\ 0 & 1 & 0 & 1/2 \\ 0 & 0 & 1 & 0 \\ 0 & 0 & 0 & 1 \end{pmatrix}, \tag{24}$$

and $\mathrm{K}_{\mathrm{Boris}} = \mathrm{K}^a_{\mathrm{Boris}} \cdot \mathrm{K}^b_{\mathrm{Boris}} \cdot \mathrm{K}^a_{\mathrm{Boris}}$ associated with the Kick. $\mathrm{K}^a_{\mathrm{Boris}}$ is half the electric part of the Kick:

$$\mathrm{K}^a_{\mathrm{Boris}} = \begin{pmatrix} 1 & 0 & 0 & 0 \\ 0 & 1 & 0 & 0 \\ -\epsilon\omega_{0x}\Delta t/2 & 0 & 1 & 0 \\ 0 & -\epsilon\omega_{0y}\Delta t/2 & 0 & 1 \end{pmatrix} \tag{25}$$

and $\mathrm{K}^b_{\mathrm{Boris}}$ the magnetic part. Using the "tan" modification:

$$\mathrm{K}^b_{\mathrm{Boris}} = \begin{pmatrix} 1 & 0 & 0 & 0 \\ 0 & 1 & 0 & 0 \\ 0 & 0 & \cos(\Omega\Delta t) & \sin(\Omega\Delta t) \\ 0 & 0 & -\sin(\Omega\Delta t) & \cos(\Omega\Delta t) \end{pmatrix} \tag{26}$$

Writing the operators in PIC form (One full drift followed by one full Kick, with $\mathbf{x}$ and $\mathbf{v}$ offset by $\Delta t/2$) would result in different propagation matrices A, but the stability conditions would not be affected.

3.2 Transversely isotropic harmonic oscillator

If $\epsilon = -1$ the elastic electrostatic force is repulsive in the ρ-direction and attractive in the **z**-direction; if in addition $\omega_{0x} = \omega_{0y} = \omega_0$ we simulate an ideal Penning trap system (See Section 4.1). When $\epsilon = 1$, the opposite holds and the particle is not axially confined (i.e. escapes on the **z**-axis); however in this section we only study the transverse stability.

Fig. (1) shows the corresponding linear stability diagrams, and a few important points should be noticed. In the absence of electric field both schemes are stable regardless of $\Omega\Delta t$. In the absence of magnetic field, both schemes are stable if $0 \leq \epsilon\omega_0\Delta t \leq 2$, which is a well known result [1]. In the limit $|\epsilon\omega_0\Delta t| \ll 1$ with $\epsilon = -1$, the scheme is unstable if $\Omega/\omega_0 < 2$: this is the physical Penning trap instability, and hence independent of the integrator (See Section 4.1 and Eq. (27)). Reliable orbit integration requires one to operate in the first stability region, containing the origin.

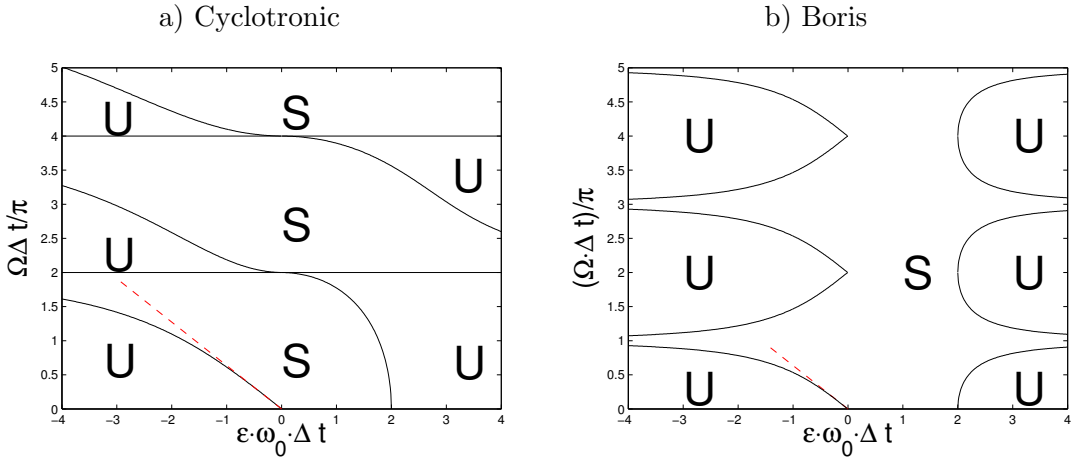

Figure 1: Linear stability diagrams for the transverse motion (the dynamics along **z** is disregarded) for the Cyclotronic (a) and the Boris (b) integrators, when the harmonic electrostatic force is transversely isotropic (Eq. (17) with $\omega_0 = \omega_{0x} = \omega_{0y}$). "S" labels stable regions, and "U" unstable regions. The red dashed line is the Penning trap instability (Eq. (27)).

3.3 Transversely one-dimensional harmonic oscillator

Let us now assume that $\omega_{0y} = 0$. The corresponding stability diagrams are shown in Fig. (2), and are slightly different from the ones in Fig. (1) although the main characteristics are similar. In is interesting to notice that the stability diagram for the Cyclotronic integrator is scaled down by a factor of 2 with respect to the $\omega_{0x} = \omega_{0y}$ case.

For arbitrary harmonic potentials ($\omega_{0x} \neq \omega_{0y}$) stability conditions are different from the ones shown in Figs (1,2). The bottom line when using either the Boris or

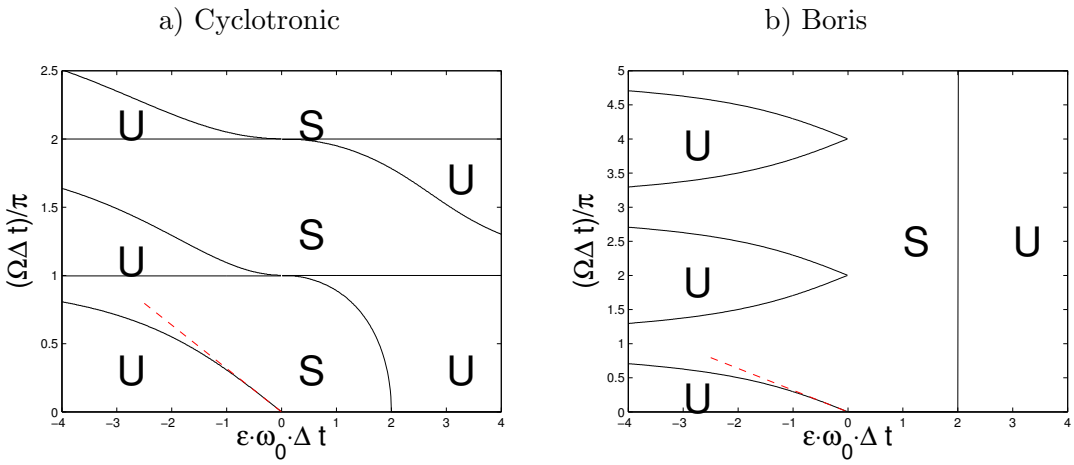

Figure 2: Linear stability diagrams for the transverse motion (the dynamics along **z** is disregarded) for the Cyclotronic (a) and the Boris (b) integrators, when the harmonic electrostatic force is transversely one-directional (Eq. (17) with $\omega_0 = \omega_{0x}$ and $\omega_{0y} = 0$). "S" labels stable regions, and "U" unstable regions. The red dashed line is a modified Penning trap stability boundary accounting for $\omega_{0y} = 0$, found to be $\Omega/\omega_0 \geq 1$.

the Cyclotronic integrator is however that in order to avoid islands of instability, the time-step should be limited to $\Omega\Delta t \lesssim 1$.

3.4 Taylor expansion algorithm of Spreiter and Walter

A previous attempt in relaxing the integrator Larmor constraint when the background magnetic field is static and uniform has been made by Spreiter and Walter [7]. Their approach, based on a Taylor expansion of the equations of motion (1) in which $\Omega\Delta t$ is not assumed to be small, yields a second-order-accurate propagation formula. It has however been pointed out by the authors that the scheme is neither symplectic nor time-reversible. In addition its Jacobian determinant is different from 1 (Jac $= 1 + O(\Delta t^4)$ in our case where the forces are conservative), which usually leads to instability [2]. It is in fact possible to verify that the scheme is unconditionally unstable for any parameters except if $\Omega\Delta t = 0$ and $0 \leq \epsilon\omega_0\Delta t \leq 2$, in which case the algorithm is merely the standard unmagnetized leap-frog [1].

As an illustration of this unconditional unstability, Fig. (3) shows contour-lines of $\delta = \max(|\mathrm{Sp}(A_{\mathrm{Tayl}})|) - 1$, where A_{Tayl} is the propagation matrix corresponding to the Taylor expansion algorithm in the presence of the electrostatic potential of Eq. (17). A_{Tayl} is easily obtained from Eqs (28-35) in Ref. [7].

The Taylor expansion algorithm can nonetheless be useful when $\Omega\Delta t \gg 1$, because in this limit $\max(|\mathrm{Sp}(A_{\mathrm{Tayl}})|$ is only slightly larger than one. Hence provided we do not need to integrate over too long a time-period the instability might not be perceptible. A more detailed comparison between this algorithm and the Cyclotronic integrator is presented in Section 8.

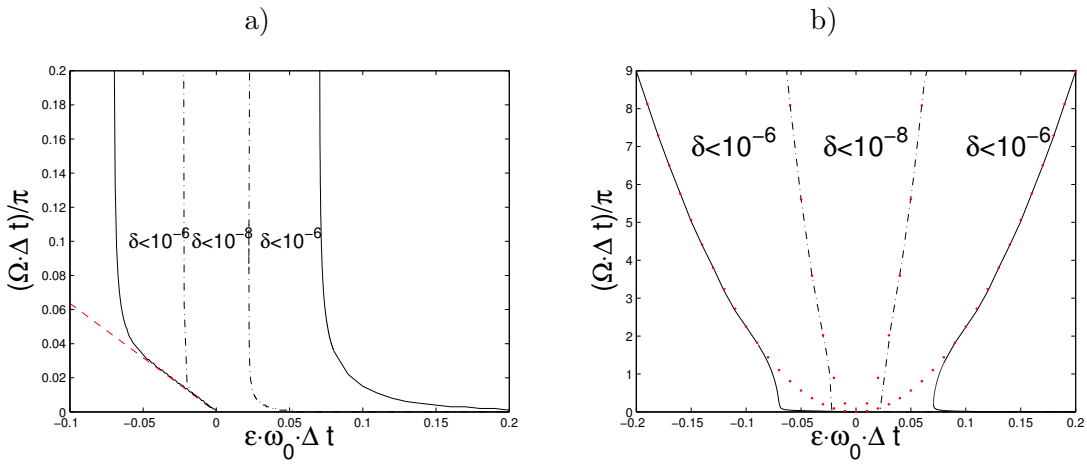

Figure 3: Contour-plots of $\delta = \max(|\mathrm{Sp}(A_{\mathrm{Tayl}})|) - 1 = 10^{-6}$ (Solid black line) and $\delta = 10^{-8}$ (Dash-dotted black line) in the vicinity of the origin (Fig. a) and for larger $\Omega\Delta t$ (Fig. b). The scheme is unconditionally unstable ($\delta > 0$) except for $\Omega\Delta t = 0$ and $0 \leq \epsilon\omega_0\Delta t \leq 2$ in which case $\delta = 0$. The red dashed line (Fig. a) corresponds to the Penning trap instability, and the red dotted parabola (Fig. b) to the large $\Omega\Delta t$ limit of the contour-lines.

4 Uniform magnetic fields: The ideal Penning trap

4.1 The ideal Penning trap

A Penning trap is a cylindrically symmetric device with a static magnetic field along the **z**-axis and a quadrupolar electrostatic field of the form of Eq. (17) with $\omega_0 = \omega_{0x} = \omega_{0y}$ and $\epsilon = 1$. Elementary algebra shows that the trap is physically stable if and only if :

$$\Omega \geq 2\omega_0 \tag{27}$$

and the the orbit is found to be a linear combination of the three following angular frequencies [12]:

$$\begin{cases} \text{Axial} & \omega_0 \\ \text{Modified Cyclotron} & \omega_{\mathrm{MC}} = \frac{\Omega}{2} + \sqrt{(\frac{\Omega}{2})^2 - \omega_0^2} \\ \text{Magnetron} & \omega_{\mathrm{Mag}} = \frac{\Omega}{2} - \sqrt{(\frac{\Omega}{2})^2 - \omega_0^2} \end{cases} \tag{28}$$

In the transverse direction the orbit is a superposition of the fast Modified Cyclotron oscillation and the slow Magnetron motion.

4.2 Frequencies shifts

Since the electric field depends linearly on the position, there is no natural scale length and one can consider the position to be dimensionless. Velocities (hence frequencies) are normalized to ω_0.

Fig. (4) shows the particle's numerically-calculated orbit projected on the **x**-axis for two different values of $\Omega\Delta t$, the only physically meaningful quantity Ω/ω_0 being kept fixed ($\Omega/\omega_0 = 10\pi/3$). Fig. (4a) corresponds to a case where Δt is six times smaller than the Larmor period ($\Omega\Delta t = \pi/3$). The 4^{th} order Runge-Kutta integrator is not satisfactory since it operates as a low-pass filter, and after a few time-steps the Cyclotron oscillation has been damped out: only the Magnetron motion is resolved. The Boris integrator resolves both frequencies but those are offset (The Magnetron frequency shift is clearly visible in the figure). The Cyclotronic integrator resolves both frequencies as well, but the error is much smaller than with the Boris integrator. Fig. (4b) corresponds to $\Omega\Delta t = 3\pi/2$, situation in which the time-step is longer than half the Larmor period. According to the Nyquist theorem this implies ω_{MC} can not be properly resolved. Examination of the Magnetron frequencies extracted from the numerical experiment (Table in Fig. (4)) shows that while the Cyclotronic integrator introduces less than 2% error, the Boris scheme is in error by a factor of 2.

a) $\Omega\Delta t = \pi/3$ b) $\Omega\Delta t = 3\pi/2$

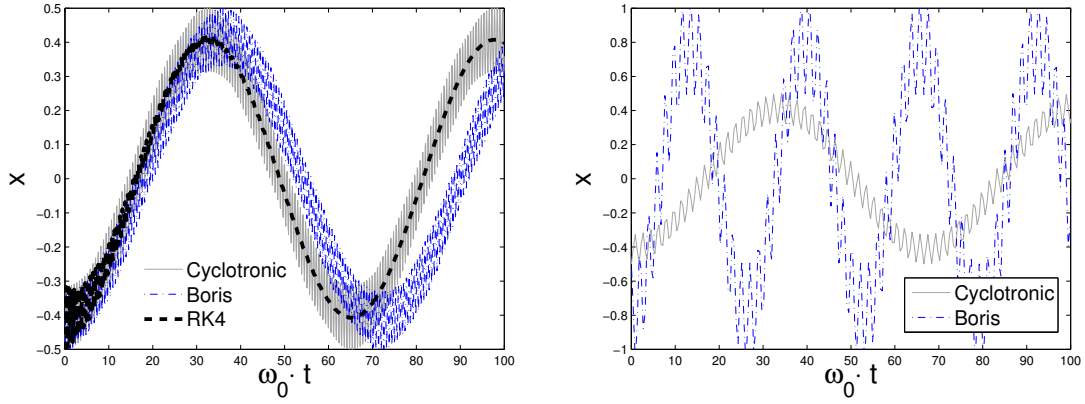

	Analytic	a (RK4)	a (Boris)	a (Cyclotronic)	b (Boris)	b (Cyclotronic)
$\omega_{\mathrm{MC}}/\omega_0$	10.38	XX	10.39	10.38	XX	XX
$\omega_{\mathrm{Mag}}/\omega_0$	$9.638 \cdot 10^{-2}$	$9.644 \cdot 10^{-2}$	$8.729 \cdot 10^{-2}$	$9.634 \cdot 10^{-2}$	0.2151	$9.782 \cdot 10^{-2}$

Figure 4: **x**-position of the particle for the Boris push, the Cyclotronic integrator and the 4^{th} order Runge-Kutta scheme, for the ideal Penning trap system. a) $\omega_0\Delta t = 0.1$ and $\Omega\Delta t = \pi/3$. b) $\omega_0\Delta t = 9/2$ and $\Omega\Delta t = 3\pi/2$. The ratio Ω/ω_0, only physically meaningful quantity, is equal in both cases ($\Omega/\omega_0 = 10\pi/3$). The initial conditions are $\mathbf{x} = (-0.5, 0, 0)$ and $\omega_0\mathbf{v} = (0, 1, 0)$. The 4^{th} order Runge-Kutta scheme does not resolve the Cyclotron motion for the parameters of Fig. a, and is unstable for the parameters of Fig. b.

Fig. (5) shows the fractional error in the characteristic frequencies ($= |(\omega_{\mathrm{Output}} - \omega_{\mathrm{Theory}})|/\omega_{\mathrm{Theory}}$) against Δt for $\Omega/\omega_0 = 5\pi/3$. Both the integrators appear second order accurate as expected, but the Cyclotronic scheme is one order of magnitude more accurate. This accuracy gap increases with the ratio Ω/ω_0, and tends to infinity if $\Omega/\omega_0 \gg 1$. If $\Omega/\omega_0 \ll 1$ both integrators become equivalent, but in no case does

the Cyclotronic integrator perform worse than the Boris scheme. The vertical dashed line in Fig. (5) shows the Nyquist limit for the Larmor frequency ($\Omega\Delta t = \pi$). For longer time-steps the Cyclotronic integrator still shows second-order accuracy for the Magnetron frequency (triangle signs).

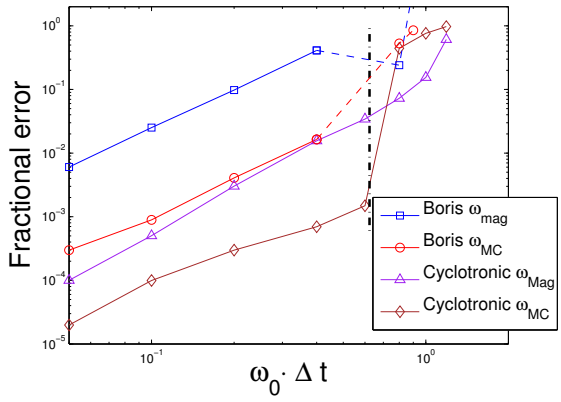

Figure 5: Fractional error on the characteristic frequencies as a function of the time-step for the Ideal Penning trap system. $\Omega/\omega_0 = 5\pi/3$.

4.3 Conservation properties

Fig. (6a) shows the particle's energy ($W = W_K + W_P$, Kinetic+Potential energy) evolution for $\Delta t = 0.1/\omega_0$. Neither of the two algorithms show a secular energy drift. Although the Boris scheme conserves energy better here than the Cyclotronic integrator, it is not a general rule and we have studied other test problems such as the magnetized Rydberg atom were the opposite holds. A careful examination of the phase-space plot in $W_K - W_P$ space (Fig. (6b)), where the red solid line has been obtained with a very small time-step and is therefore considered to be the "exact" trajectory, shows that for the Boris push the velocity and position errors are higher than for the Cyclotronic integrator (the "+" signs span a more accurate length of the solid line), but compensate themselves in a better fashion (The "o" signs align themselves with the solid line better than the "+" signs). The 4^{th} order Runge-Kutta scheme does not conserve energy.

Fig. (7) shows the Canonical angular momentum conservation (Eq. (11)) for the same parameters as in Fig. (6). When using the Cyclotronic integrator p_φ is exactly conserved. Indeed the Drift (Eq. (15)) is the mapping of a Larmor rotation and by definition conserves p_φ, and because of the cylindrical geometry of the potential the Kick (Eq. (16)) doesn't change v_φ. As expected the Boris integrator introduces an error in p_φ but no secular drift as opposed to the 4^{th} order Runge-Kutta scheme.

a) Energy in time space

b) Energy in $W_K - W_P$ space

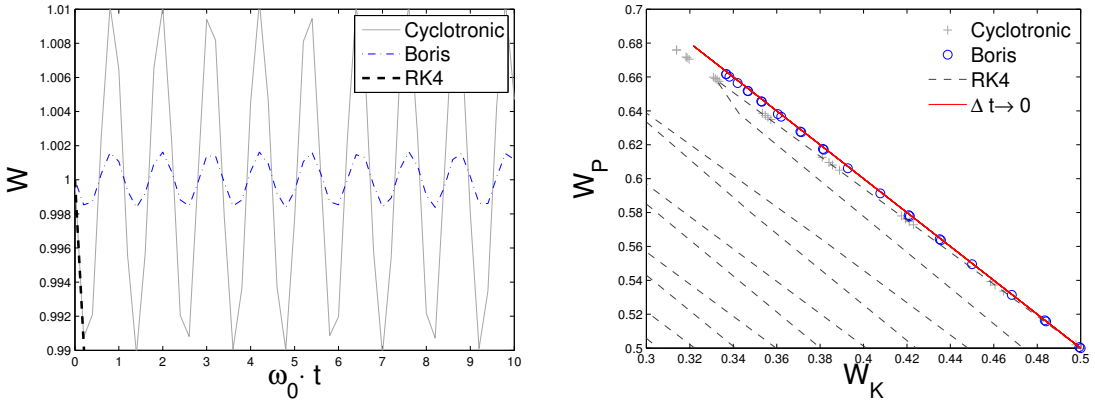

Figure 6: Fig.a shows the time evolution of the energy for the ideal Penning trap system, with $\Omega\Delta t = \pi/3$ and $\omega_0\Delta t = 0.2$. The initial conditions are $\mathbf{x} = (1, 0, 0)$ and $\omega_0\mathbf{v} = (1, 0, 0)$. Fig. b illustrates the particle evolution in $W_K - W_P$ (Kinetic and Potential energy) space.

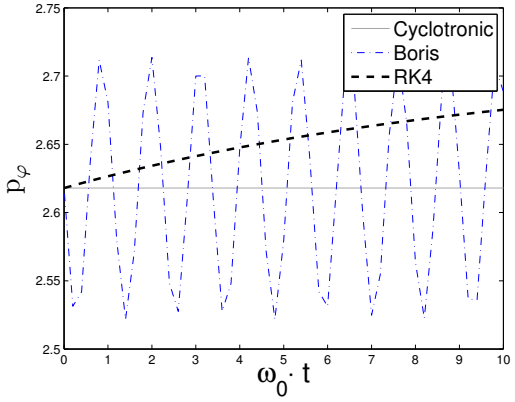

Figure 7: Canonical angular momentum evolution for the same system and parameters as in Fig. (6).

4.4 Comparison of the Taylor expansion algorithm and the Cyclotronic integrator

Although unconditionally unstable, it is interesting to compare the Taylor expansion algorithm described in Section 3.4 with the Cyclotronic integrator. We do so for the ideal Penning Trap system, since both schemes are optimal for static uniform magnetic fields.

Fig. (8a) shows the particle position projected on the **x**-direction with parameters $\Omega\Delta t = \pi$ and $\omega_0\Delta t = 0.2$, with initial conditions $\mathbf{x} = (-0.5, 0, 0)$ and $\omega_0\mathbf{v} = (0, 1, 0)$. While the trajectory computed using the Cyclotronic integrator is bounded, such is not the case when using the Taylor expansion algorithm, which is clearly a handicap if long-term integration is needed. As shown in Fig. (8b) both schemes compute the same characteristic frequencies; the spectrum associated with the Taylor expansion algorithm is however polluted by its instability.

a) **x**-position in time space

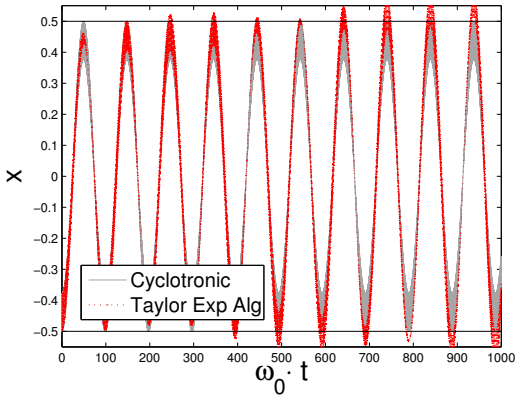

b) **x**-position in frequency space

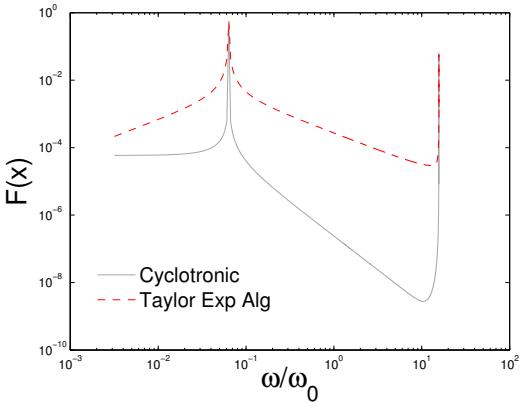

Figure 8: Fig. a shows the **x**-position evolution with time for the ideal Penning trap system, with $\Omega\Delta t = \pi$ and $\omega_0\Delta t = 0.2$. The initial conditions are $\mathbf{x} = (-0.5, 0, 0)$ and $\omega_0\mathbf{v} = (0, 1, 0)$. Fig. b is the Fourier transform of Fig. a carried on 20 Magnetron periods. The high frequency peak has little meaning since the sampling frequency is exactly equal to the Nyquist frequency for the Larmor motion. The low angular frequency peak (Magnetron frequency) is identical for both the Cyclotronic integrator and the Taylor expansion algorithm. The unstability of the Taylor expansion algorithm appears in Fig b as the non negligible Fourier weigth of non resonant frequencies.

5 Non-uniform magnetic fields: The non-ideal Penning trap

5.1 The non-ideal Penning trap

The Cyclotronic integrator has been shown to be symplectic only for a uniform magnetic field and even a slight excursion from this condition ruins the integrator properties. In particular, a straightforward examination of Eqs (15,16) shows that if the magnetic field is non-uniform the scheme is not even time-reversible. This is not the case for the Boris push, which is time-reversible regardless of the magnetic geometry.

For illustration purposes, we consider a non ideal Penning trap where the electrostatic potential is still given by Eq. (17) with $\omega_0 = \omega_{0z} = \omega_{0y}$, but the magnetic field by the following simplified Helmholtz coils formula:

$$\left\{ \begin{array}{rcl} B_z & = & B_z(0)\frac{5\sqrt{5}}{16}\left[\frac{1}{(1/2+(z/R)^2)^{3/2}} + \frac{1}{(-1/2+(z/R)^2)^{3/2}}\right] \\ \mathbf{B}_\rho & = & -\frac{\rho}{2}\frac{\partial B_z}{\partial z}\mathbf{e}_\rho, \end{array} \right. \tag{29}$$

where R is the coils radii. Of course Eq. (29) is only valid close to the axis, but we here use it in the entire space.

Because $\mathbf{B}$ is not uniform the problem loses its linearity, and the position becomes dimensional. We here measure lengths in units of $x_0 = x(0)$, the $\mathbf{x}$-position of the particle at $t = 0$. We also define $\Omega_0 = QB_z(0)/m$.

5.2 Numerical experiments

Fig. (9) illustrates the results of numerical experiments with $\omega_0\Delta t = 0.2$ and $\Omega_0\Delta t = \frac{2\pi}{3}$. Fig. (9a) confirms that the Cyclotronic integrator does not ensure energy conservation in non-uniform magnetic field conditions, while the Boris scheme does. If the time-step is reduced by a factor of 10, the energy excursion introduced by Boris scheme is approximately reduced by a factor of 240, which is the right order of magnitude for a second order scheme.

Fig. (9b) shows the particle trajectory projected in the $\mathbf{x}$-direction for the same parameters, and using the Cyclotronic integrator one finds that it nonphysically converges towards x=0. It is however interesting to notice that although the Cyclotronic scheme does not behave appropriately in the long-term, it still resolves the Magnetron frequency more accurately than the Boris push (ω_{Mag} computed using the Cyclotronic integrator with Δt is very close to the one computed using the Boris scheme and $\Delta t/10$).

6 Summary

The orbit integrator is a key ingredient in Particle in Cell codes and special care must be used in its choice, in particular because particle advance is usually the most

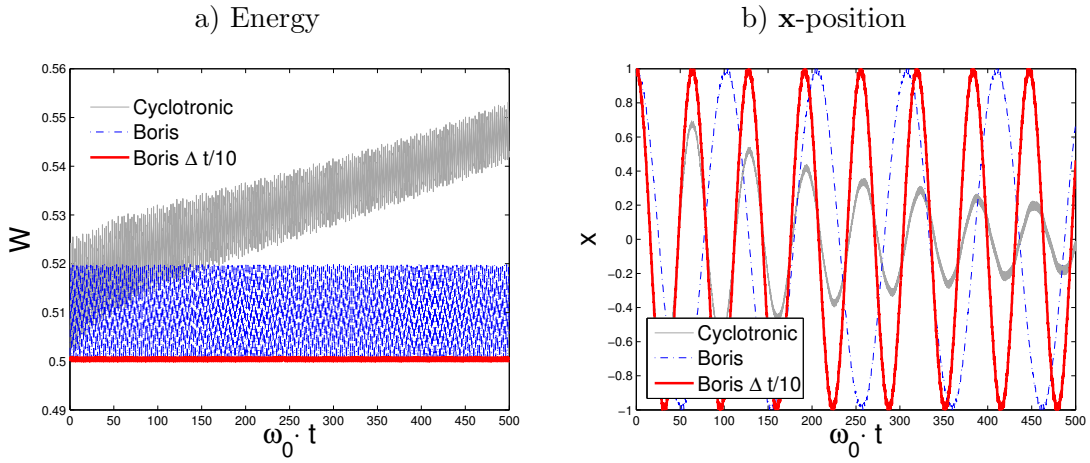

Figure 9: Energy (Fig. a) and **x**-position (Fig. b) evolution with time for the non ideal Penning trap system with magnetic field given by Eq. (29). The simulation parameters are $R = 2$, $\omega_0 \Delta t = 0.2$ ("Cyclotronic" and "Boris" labels) and $\Omega_0 \Delta t = \frac{2\pi}{3}$. The red thick curve labeled $\Delta t/10$ corresponds to the Boris integrator with $\omega_0 \Delta t = 0.02$ and $\Omega_0 \Delta t = \frac{2\pi}{30}$. The initial conditions are $\mathbf{x} = (1, 0, 0)x_0$ and $\omega_0 \mathbf{v} = (0, 0, 0)x_0$.

expensive step. The present publication is devoted to explicit schemes in the presence of a background magnetic field.

Because it is time-reversible, the Boris integrator (Eqs (2,3)) is well known for its long term conservation properties in any magnetic field geometry. It is also linearly stable for reasonably small time-teps, as shown in Figs (1,2). It however suffers from the need to accurately resolve the Larmor frequency, which is inefficient if it is much larger than any other characteristic frequencies of the problem.

In order to dodge the Larmor constraint, Spreiter and Walter developed a particle mover whose truncation error is independent of the strength of the magnetic field provided it is constant and uniform (Section 3.4). This algorithm is definitely useful if the problem allows it to be used with a time-step much longer than the Larmor period [13], but too unstable when this is not the case (Fig. (3)). In addition it does not exactly conserve energy, which could be a problem if used in codes where long-term particle tracking is necessary.

The central message of this publication is that we have developed a new second order orbit integrator not subject to the Larmor constraint, which is symplectic (Hence time-reversible) when the magnetic field is static and uniform. Provided the non-magnetic characteristic frequencies are accurately enough resolved, it is only subject to a stability constraint (The time step must be smaller than half a Larmor period, see Figs (1,2)). It can of course also be used with smaller time-steps as opposed to the algorithm of Spreiter and Walter. This Cyclotronic integrator can easily be implemented in leap-frog style (Position and velocity offset by half a time-step), as illustrated by Eqs (16,15). When applied to non-uniform magnetic fields its conservation properties are lost; however some features such as the Magnetron frequencies in non ideal Penning

traps are still more accurately captured than with the Boris scheme.

The Cyclotronic integrator has successfully been implemented in the electrostatic PIC codes SCEPTIC [4, 5] and in recent versions of Democritus [14].

Acknowledgments

Leonardo Patacchini was supported in part by NSF/DOE Grant No. DE-FG02-06ER54891. The SCEPTIC calculations are performed on the Alcator Beowulf cluster which is supported by U.S. DOE Grant No. DE-FC02-99ER54512. The implementation of the Cyclotronic integrator in Democritus was performed in collaboration with Giovanni Lapenta.

References

[1] C. Birdsall A. Langdon *Plasma Physics via computer simulation* McGraw Hill New York (1985).

[2] V. Fuchs and J.P. Gunn *On the integration of equations of motion for particle-in-cell codes* Journal of Computational Physics **214** pp 299-315 (2006).

[3] R.I. McLachlan and M. Perlmutter *Energy drift in reversible time integration* Letter to the Editor, Journal of Physics A, **37** 45, (2004).

[4] L. Patacchini and I.H. Hutchinson *Angular distribution of current to a sphere in a flowing, weakly magnetized plasma with negligible Debye length* Plasma Phys. Control. Fusion **49** pp 1193-1208 (2007).

[5] L. Patacchini and I.H. Hutchinson *Ion-collecting sphere in a stationary, weakly magnetized plasma with finite shielding length* Plasma Phys. Control. Fusion **49** pp 1717-1733 (2007).

[6] D. Donnelly and E. Rogers *Symplectic integrators: An introduction* Am. J. Phys., **73** 10 (2005).

[7] Q. Spreiter and M. Walter *Classical Molecular Dynamics Simulation with the Velocity Verlet Algorithm at Strong External Magnetic Fields* Journal of Computational Physics **152** pp 102-119 (1999).

[8] H. Kinoshita, H. Yoshida and H. Nakai *Symplectic integration and their application to dynamical astronomy* Celestial Mechanics and Dynamical Astronomy **50** pp 29-71 (1991).

[9] E. Forest *Geometric integration for particle accelerators* J. Phys A **39** 5321-5377 (2006).

[10] P.G. Hjorth and N. Nordkvist *Classical Mechanics and Symplectic Integration* Unpublished notes available on line : *http* : *//www2.mat.dtu.dk/people/N.Nordkvist/lecture_notes.pdf*

[11] P.H. Stolz and al. *Efficiency of a Boris-like integration scheme with spatial stepping* Physical Review Special Topics - Accelerators and beams **5**, 094001 (2002).

[12] L.S. Brown and G. Gabrielse *Geonium theory: Physics of a single electron or ion in a Penning trap* reviews of modern physics **58** pp 233-311 (1986).

[13] F. Herfurth, S. Eliseev and al. *The HITRAP project at GSI: trapping and cooling of highly-charged ions in a Penning trap* Hyperfine Interactions **173** pp 1-3 (2006).

[14] G. Lapenta *Simulation of Charging and Shielding of Dust Particles in Drifting Plasmas* Physics of Plasmas **6** pp 1442-1447 (1999).